

See discussions, stats, and author profiles for this publication at: <https://www.researchgate.net/publication/280240947>

# Advancing Model Systems for Fundamental Laboratory Studies of Sea Spray Aerosol Using the Microbial Loop

ARTICLE *in* THE JOURNAL OF PHYSICAL CHEMISTRY A · JULY 2015

Impact Factor: 2.69 · DOI: 10.1021/acs.jpca.5b03488 · Source: PubMed

CITATION

1

READS

74

## 13 AUTHORS, INCLUDING:



Jessica Axson

University of Michigan

21 PUBLICATIONS 99 CITATIONS

SEE PROFILE



Francesca Malfatti

University of California, San Diego

23 PUBLICATIONS 554 CITATIONS

SEE PROFILE



Grant B. Deane

University of California, San Diego

137 PUBLICATIONS 1,174 CITATIONS

SEE PROFILE



Kim Prather

University of California, San Diego

295 PUBLICATIONS 9,729 CITATIONS

SEE PROFILE

# Advancing Model Systems for Fundamental Laboratory Studies of Sea Spray Aerosol Using the Microbial Loop

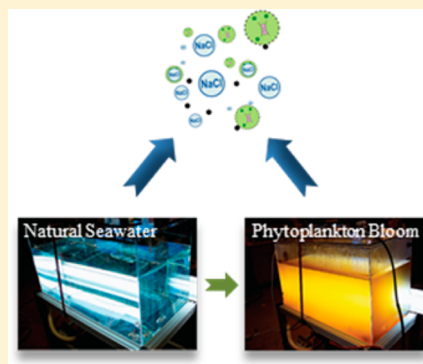
Christopher Lee,<sup>†</sup> Camille M. Sultana,<sup>†</sup> Douglas B. Collins,<sup>†</sup> Mitchell V. Santander,<sup>†</sup> Jessica L. Axson,<sup>†,Δ</sup> Francesca Malfatti,<sup>‡,▽</sup> Gavin C. Cornwell,<sup>†</sup> Joshua R. Grandquist,<sup>§</sup> Grant B. Deane,<sup>‡</sup> M. Dale Stokes,<sup>‡</sup> Farooq Azam,<sup>‡</sup> Vicki H. Grassian,<sup>§,||</sup> and Kimberly A. Prather<sup>\*,†,‡</sup>

<sup>†</sup>Department of Chemistry and Biochemistry and <sup>‡</sup>Scripps Institution of Oceanography, University of California, San Diego, California 92093, United States

<sup>§</sup>Department of Chemical and Biochemical Engineering and <sup>||</sup>Department of Chemistry, University of Iowa, Iowa City, Iowa 52242, United States

## S Supporting Information

**ABSTRACT:** Sea spray aerosol (SSA) particles represent one of the most abundant surfaces available for heterogeneous reactions to occur upon and thus profoundly alter the composition of the troposphere. In an effort to better understand tropospheric heterogeneous reaction processes, fundamental laboratory studies must be able to accurately reproduce the chemical complexity of SSA. Here we describe a new approach that uses microbial processes to control the composition of seawater and SSA particle composition. By inducing a phytoplankton bloom, we are able to create dynamic ecosystem interactions between marine microorganisms, which serve to alter the organic mixtures present in seawater. Using this controlled approach, changes in seawater composition become reflected in the chemical composition of SSA particles 4 to 10 d after the peak in chlorophyll-*a*. This approach for producing and varying the chemical complexity of a dominant tropospheric aerosol provides the foundation for further investigations of the physical and chemical properties of realistic SSA particles under controlled conditions.



## 1. INTRODUCTION

Seminal studies by Professor Mario J. Molina and co-workers demonstrated the profound influence heterogeneous reactions can have on the composition of the stratosphere. These studies provided an exemplary example of how laboratory studies of fundamental physical chemistry can play an essential role in explaining atmospheric observations,<sup>1–3</sup> ultimately providing solutions to complex environmental problems. Laboratory studies simulated the composition of stratospheric aerosol particles comprised of ice, nitric acid, and ammonium sulfate.<sup>4,5</sup> The studies, which elucidated the detailed mechanisms involving surface adsorption and chemistry,<sup>3</sup> led to the understanding of their climatic effects and lifetime in the stratosphere.<sup>6</sup>

Compared to stratospheric aerosols, tropospheric aerosols are chemically far more complex. They originate from a wide range of natural and anthropogenic sources, can be comprised of multiple phases, and contain thousands of compounds, including complex mixtures of organic and inorganic species.<sup>7,8</sup> Sea spray aerosol (SSA) particles are generated at the ocean surface by breaking waves and bursting of whitecap foam bubbles<sup>7,9,10</sup> and constitute one of the most abundant aerosol particle types in the atmosphere.<sup>7,8,11</sup> Previous studies have suggested that the organic fraction of SSA in the marine

boundary layer increases during periods of high biological activity in the ocean.<sup>12</sup> Understanding the factors controlling these changes is important as inclusion of organic material in SSA particles has been shown to influence water uptake,<sup>13,14</sup> heterogeneous nucleation of ice,<sup>15,16</sup> and chemical reactivity with important atmospheric trace gases.<sup>17,18</sup>

The initial studies by Molina and co-workers on stratospheric aerosol particles demonstrated how controlled fundamental studies were essential for understanding and solving large-scale atmospheric phenomena.<sup>19–22</sup> Since these early studies, fundamental physical chemistry investigations have probed tropospheric SSA particles<sup>17,23</sup> using model SSA systems comprised of sodium chloride mixed with organic species such as sodium dodecyl sulfate.<sup>24–26</sup> While studies using model systems have provided critical insights into the behavior of mixtures of organic and inorganic species, they cannot be used to explain reactions that occur on chemically complex naturally produced SSA particles. Accurately replicating tropospheric aerosols so that laboratory study results can be used to explain atmospheric observations represent an enormous challenge as

Received: April 10, 2015

Revised: July 20, 2015

Published: July 21, 2015



the interfacial properties and overall chemical composition of SSA particles depend in a poorly understood way on seawater composition and sea spray production mechanisms.<sup>27,28</sup>

Breaking waves lead to a unique production mechanism that ultimately produces SSA particles.<sup>28,29</sup> Efforts have been made to replicate the same physical mechanisms for SSA particle production in the laboratory through the development of the Marine Aerosol Reference Tank (MART), a portable system with ability to produce a similar set of bubble sizes to breaking waves that are critical to replicating the size distribution and chemical mixing state of SSA generated by wave breaking.<sup>27,29</sup> While previous studies have investigated the effect serial additions of representative microorganism cultures and organic molecules to seawater has on SSA chemical and physical properties,<sup>27,28,30</sup> it is impossible to replicate the full complexity of the myriad of organic molecules present in ambient seawater using this method. The novelty of this study involves developing a protocol for reproducing the natural chemical complexity inherent to biologically active regions of the oceans by utilizing phytoplankton blooms to induce a change in the seawater composition and the resulting SSA. The interactions between phytoplankton, bacteria, and viruses present in the seawater produce a complex mixture of organic molecules that closely represent surface ocean biochemical conditions.

This study illustrates how one can use microbial processes to produce a chemically complex suite of organic compounds such as those produced in the ocean<sup>31–35</sup> for more realistic studies of isolated SSA physical and chemical properties. Figure 1A shows

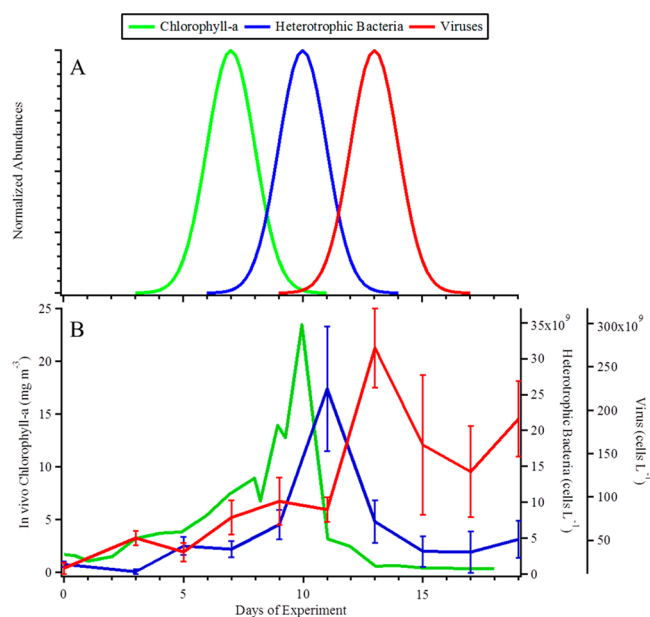


**Figure 1.** Evolution of phytoplankton as chlorophyll-a, heterotrophic bacteria, and virus concentrations for an idealized microcosm (panel A) vs data (panel B) from a representative experiment (data from Tank B).

an idealized scheme of the dynamics of marine microorganisms within a phytoplankton bloom microcosm experiment. Phytoplankton reduce CO<sub>2</sub> and represent a source of dissolved organic carbon (DOC) in the seawater. This organic matter is further transformed and processed by interactions with marine microorganisms such as heterotrophic bacteria.<sup>32,34–36</sup> The natural synthesis and subsequent chemical processing of organic compounds by marine microorganisms allows the

complexity of ocean chemistry to be replicated in a manner that mimics naturally occurring ocean processes that ultimately influence the composition of ejected SSA particles, affecting water uptake and reactivity. Fundamental studies of the physicochemical properties of SSA particles can then be performed in a controlled environment on aerosol particles that closely resemble those produced in the natural environment.<sup>27</sup>

## 2. EXPERIMENTAL METHODS

### 2.1. Marine Aerosol Reference Tank Photobioreactor Configuration.

High-definition fluorescent tubes (Full Spectrum Solutions, model 205457) with a blackbody radiation temperature of 5700 K, to closely mimic the radiation profile of the sun, were mounted to the MART to irradiate the seawater and stimulate the growth of marine phytoplankton (Figure S1). These lights were positioned to generate  $\sim 70 \mu\text{E m}^{-2} \text{s}^{-1}$  photosynthetically active radiation (PAR; Apogee Instruments, MQ-200) measured at  $\sim 15$  cm below the surface of the seawater in the MART. Summer noon surface PAR levels have been reported from satellite observations to be from  $\sim 1000$  to  $1500 \mu\text{E m}^{-2} \text{s}^{-1}$  regularly between  $40^\circ \text{N}$  and  $40^\circ \text{S}$ ,<sup>37</sup> whereas the much lower experimental irradiance condition used in this study simulates the radiation flux density typically used in the growth of phytoplankton cultures.<sup>38,39</sup> Constant PAR illumination at the level used in this study allowed steady and controlled growth of phytoplankton in the MART.

Natural seawater collected at the end of Scripps Pier (La Jolla, CA;  $32^\circ 52' 00'' \text{N}$ ,  $117^\circ 15' 21'' \text{W}$ ; 275 m offshore) was filtered using  $50 \mu\text{m}$  Nitex mesh (Sefar Nitex 03–100/32) and added to the MART (ocean conditions at the time of seawater sampling listed in Table S1). After a 24 h temperature adjustment period, phytoplankton growth was stimulated by adding diatom growth medium commonly known as Guillard's f medium (ProLine Aquatic Ecosystems) diluted by a factor of 2 (f/2) or by a factor of 20 (f/20) including Na<sub>2</sub>SiO<sub>3</sub> (full list of components and concentrations listed in Table S2).<sup>40,41</sup> The biological community and the chemical composition of the collected seawater were not controlled or adjusted prior to the addition of diatom growth medium with the exception of filtering large phytoplankton predators known as grazers using the Nitex mesh filter;<sup>32,35</sup> thus, the starting conditions are referred to as "unconstrained." A bubbler system of Tygon tubing and glass weights was then placed on the bottom of the MART to provide gentle mixing and aeration until in vivo chlorophyll-a concentrations reached  $\sim 12 \text{ mg m}^{-3}$ .

The threshold of  $12 \text{ mg m}^{-3}$  was chosen to be the time to begin using the SSA particle production mechanism as studies found that the water recirculation system used to produce the plunging waterfall could inhibit the phytoplankton growth. This was attributed to the lysing of phytoplankton cells by the high shear force of the mechanical pump used to circulate the seawater through the plunging waterfall aerosol generation apparatus. Once the chlorophyll-a concentration reached the threshold, the bubbler system was removed and SSA particle generation was started through pulsed plunging waterfall technique with 4 s waterfall duty cycle.<sup>29</sup> SSA particles were generated and analyzed during 2 h periods followed by 2 h with no particle generation or mixing. This "2 h on, 2 h off" protocol was implemented as a compromise to allow the biological processes in the seawater to thrive while providing enough SSA particles to sample. Operating the mechanical pump for SSA particle generation past this threshold for 2 h did not affect

chlorophyll-*a* concentrations. The chlorophyll-*a* concentration continued to increase for several (2–4) days after particle generation resumed, thus suggesting that even with the mechanical pump, some phytoplankton populations were still able to bloom. A total of six MART microcosm experiments were conducted in this study to explore the variability due to the lack of chemical/biological constraint on the initial seawater sample; full details can be found in the [Supporting Information](#).

**2.2. Chemical and Biological Measurements of Seawater.** Subsurface bulk seawater was collected through a stainless steel valve mounted ~20 cm below the surface of the seawater on the tank. To sample the sea surface microlayer (SML), the glass plate method was utilized as this technique allowed efficient collection of the large volume needed for microscopic analysis from the upper 100  $\mu\text{m}$  of the sea surface.<sup>42</sup> Aerosol impingers (Chemglass, CG-1820, 0.2  $\mu\text{m}$   $D_p$  lower cutoff) were used to collect SSA particles for quantification of ejected marine microorganisms and chemical characterization of aerosolized organic matter by fluorescence spectroscopic methods. Throughout the course of the microcosm experiment, daily measurements of the bulk DOC concentration and in vivo chlorophyll-*a* fluorescence were made. In vivo chlorophyll-*a* fluorescence, measured by a commercial portable fluorimeter (Aquafluor, Turner Designs), was used to track phytoplankton biomass. For determination of DOC concentrations, a metric used to quantify dissolved organic matter (DOM), bulk seawater was passed through a 0.7  $\mu\text{m}$  filter (Whatman GF/F, Z242489) and immediately acidified with two drops of trace metal-free 12 N HCl to approximately a pH of 2. The sample was then analyzed using the high-temperature combustion method (Shimadzu Scientific Instruments, TOC-V CSN).<sup>43</sup> The same filtering process was performed to filter the seawater for fluorescence excitation–emission matrix (EEM) spectroscopy (Horiba Scientific, Aqualog) to characterize and obtain relative concentration of fluorescent organic compounds. Optical counts of marine bacteria and viruses in the bulk, SML, and impinged SSA particles in sterile seawater were performed using epifluorescence microscopy (Olympus, IX71) with SYBR Green-I nucleic acid gel stain (Life Technologies, S-7563) where bacteria and viruses were discriminated based on their size.<sup>44</sup>

**2.3. Chemical Measurements of Sea Spray Aerosol Particles.** Under the typical operating conditions for this study, the headspace of the MART during SSA particle generation had a relative humidity (RH) greater than 90% (Vaisala, HMP110) with a residence time less than 15 min at an air flow rate of 6 SLPM. The relatively short residence time led to sampling primary SSA particles,<sup>24</sup> as secondary (gas-particle) chemistry processes such as secondary aerosol formation are slower than the average lifetime in the headspace.<sup>45,46</sup> The size-resolved chemical compositions of individual SSA particles ranging from 0.3 to 3.0  $\mu\text{m}$  in vacuum aerodynamic diameter ( $D_{va}$ ) were measured in real time using an aerosol time-of-flight mass spectrometer (ATOFMS). More detailed information on this analytical technique can be found elsewhere,<sup>47</sup> but briefly, particles are drawn through a nozzle inlet and are accelerated through two stages of differential pumping, wherein each particle reaches its size-dependent terminal velocity. Particles pass through two orthogonally positioned diode-pumped solid-state continuous wave lasers (CrystaLaser, diode-pumped Nd:YAG, 532 nm, 50 mW). The transit time of the particle between the two lasers is used to determine particle velocity.  $D_{va}$  is calculated for each particle using a calibration curve

generated using polystyrene latex spheres of known diameter and density. The velocity is also used to trigger a pulsed, Q-switched Nd:YAG laser at 266 nm (Quantel, 8 ns pulse width, 700  $\mu\text{m}$  spot size,  $3 \times 10^7 \text{ W cm}^{-2}$ ) which desorbs and ionizes each particle. Simultaneous acquisition of both positive and negative ion mass spectra for individual particles was obtained using a dual polarity reflectron time-of-flight mass spectrometer with microchannel plate detectors (Photonis, 931377). Collected data were imported into MATLAB (The MathWorks, Inc.) with software toolkit YAADA ([www.yaada.org](http://www.yaada.org)) for further data analysis.

MART-generated SSA particles were collected for further offline analysis of physical and chemical composition using a Micro Orifice Uniform Deposit Impactor (MOUDI, MSP Corp. model 100-NR, 10 stages) and aerosol impingers. The MOUDI allows size-fractionated particle samples to be collected. SSA particles (aerodynamic diameter range from 0.56 to 1.0  $\mu\text{m}$ ) collected on Si wafer substrates (Ted Pella Inc., 16008) mounted in the MOUDI on stage 6 (aerodynamic diameter range of 0.56–1.0  $\mu\text{m}$ ) were analyzed using scanning electron microscopy (SEM; Hitachi S-4800, 5 kV accelerating voltage, 15  $\mu\text{A}$ , 10 $\times$  magnification). Aerosol impingers filled with ultrapure water were used to collect SSA particles for further analysis through fluorescence EEM spectroscopy.

### 3. RESULTS AND DISCUSSION

**3.1. Validation of Marine Aerosol Reference Tank and Ambient Measurements.** Comparison of the laboratory approach in this study to ambient measurements served as a test of how closely laboratory-generated SSA resembled atmospheric aerosols. The chemical compositions of particles generated from the MART microcosm experiments were compared to ambient data collected at Bodega Bay, CA (Bodega Marine Laboratory, 38° 18' 13" N, 123° 03' 52" W). A period during which clean marine air arrived at the coastal sampling site from the oceanic northwestern sector with minimal contributions from anthropogenic sources verified by particle chemical analysis by ATOFMS (March 17, 2015, 10:00 to 21:00; wind from 313°  $\pm$  6°, 12.3  $\pm$  1.7  $\text{m s}^{-1}$ ) was used for comparison with SSA particles generated from natural seawater in a MART prior to addition of any nutrients. The surface ocean surrounding Bodega Bay had elevated biological activity during the time of sampling (~2  $\text{mg m}^{-3}$  in chlorophyll-*a* concentration observed from MODIS, [Figure S2](#)). Ambient particles were sampled in real time and were chemically classified based on their dual-polarity mass spectra using criteria previously established<sup>28</sup> and described below. MART tank D was chosen for this intercomparison due to the similarity of chlorophyll-*a* concentrations (~2  $\text{mg m}^{-3}$ ) with those during the study at Bodega Bay.

Real-time measurements of single SSA particle chemical composition using ATOFMS have revealed a number of particle types enriched in organic components.<sup>28,48,49</sup> [Figure S3](#) shows the representative mass spectra of three distinct types of SSA particles observed in these experiments. Three main classifications of SSA particles were determined: sea salt (SS), sea salt mixed with organic carbon (SS-OC), and a biological type consisting of  $\text{Mg}^{2+}$  coupled with organic-nitrogen species (Biological), consistent with the SSA types reported previously.<sup>28,48</sup> The SS type consists of particles containing dominant ion markers for sodium and chloride ( $^{23}\text{Na}^+$  and  $^{35,37}\text{Cl}^-$ ) with sodium chloride ion clusters observed at  $^{81,83}\text{Na}_2\text{Cl}^+$  and  $^{93,95,97}\text{NaCl}_2^-$  and a minor signal from  $^{24}\text{Mg}^+$



and  $^{39}\text{K}^+$ . The SS-OC type closely resembled the signature of the SS type but with elevated signal from  $^{24}\text{Mg}^+$ ,  $^{39}\text{K}^+$ ,  $^{26}\text{CN}^-$ , and  $^{42}\text{CNO}^-$  with a minor contribution from  $^{79}\text{PO}_3^-$ . Biological-type spectra were dominated by  $^{24}\text{Mg}^+$  ion signal with contributions from  $^{39}\text{K}^+$ ,  $^{129,131,133}\text{MgCl}_3^-$ ,  $^{35,37}\text{Cl}^-$ ,  $^{26}\text{CN}^-$ ,  $^{42}\text{CNO}^-$  and  $^{79}\text{PO}_3^-$ . A detailed analysis of the SS-OC and biological particle types, abundances, and association with the composition of the seawater will be described in a separate manuscript.

During the clean marine period, a small fraction ( $\sim 11\%$ ) of the particles sampled at Bodega Bay showed signs of atmospheric chemical processing due to the presence of nitrate ion markers ( $^{46}\text{NO}_2^-$ ,  $^{62}\text{NO}_3^-$ ),<sup>50</sup> where during other periods, fractions of atmospherically aged particles ranged from 20 to 80%. The fractions of SS-OC and Biological particles compared to SS from the clean marine period ambient measurements were similar to those produced in the MART experiments for the size range measured by the ATOFMS ( $0.3$  to  $3.0\ \mu\text{m}\ D_{\text{va}}$ ). The ambient particle fraction of both laboratory and field studies examining marine systems show a large SS dominance, followed by Biological- and SS-OC-type particles (Figure 2).

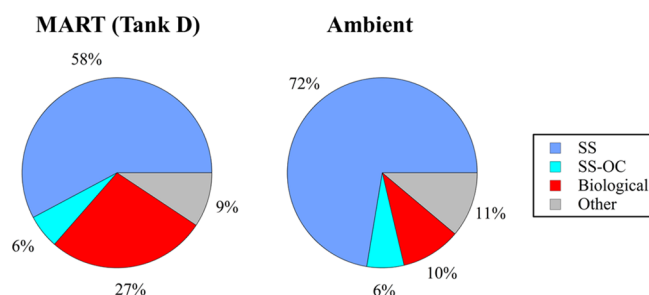


**Figure 2.** Comparison of particle-type fractions observed in a MART microcosm (left) and ambient marine aerosols during a clean atmospheric period at Bodega Bay, CA. MART measurements were made prior to media addition. On the basis of individual particle composition, particles are categorized into sea salt (SS), sea salt-organic carbon (SS-OC), Biological, and other.

The variations can be attributed to the difference in ocean conditions and organic concentrations in the bulk seawater and the SML, as the organic enrichment in SSA particles depends on the state of biological cycle as discussed below. Despite differences in seawater conditions, the MART microcosm showed remarkable similarity in particle types and mixing state to those observed in ambient air at a coastal site during onshore flow. SSA particles greater than  $1\ \mu\text{m}$  in diameter ( $D_p$ ) are sensitive to secondary processing such as heterogeneous chemistry due to large surface area to unit volume available.<sup>24,51</sup>

As ATOFMS is sensitive in distinguishing the extent of atmospheric processing in the size that would have the significant impact ( $1\text{--}3\ \mu\text{m}\ D_p$ ), the generation of SSA from natural unconstrained seawater using a realistic particle production mechanism in the isolated MART system overall replicates primary SSA particles observed in the atmosphere. Isolating natural SSA produced using the proper physical and biological mechanisms will allow controlled laboratory studies of the heterogeneous reaction of natural sea spray particles without competing effects from anthropogenic sources.

**3.2. Simulating the Biological Chemical Engine in the Marine Aerosol Reference Tank.** Six phytoplankton microcosm experiments were conducted to determine the reproducibility and natural variability in the seawater and SSA

composition using this approach. Despite the unconstrained starting conditions of each experiment, in vivo chlorophyll-a measurements showed that the phytoplankton blooms had similar temporal behavior. Figure S4 shows a compilation of chlorophyll-a concentration measurements normalized to each respective maximum chlorophyll-a concentration. In these microcosm experiments, peak chlorophyll-a concentrations ranging from  $25$  to  $59\ \text{mg}\ \text{m}^{-3}$  were achieved using  $f/2$  and  $f/20$  nutrient concentrations, thus providing a range of chlorophyll-a concentrations for the systematic study of seawater bio-geochemistry on SSA (Figure S4). Typical phytoplankton blooms in the oceans have been observed from  $\sim 1$  to  $70\ \text{mg}\ \text{m}^{-3}$  chlorophyll-a.<sup>52–56</sup> Although the observed peak chlorophyll-a concentrations from the microcosms were within the range of observed oceanic phytoplankton blooms,<sup>54</sup> having this higher level of biological activity will lead to larger more easily measured changes in SSA composition. Overall, studies on SSA produced from MART microcosms will be useful for understanding how changes in SSA composition affects SSA particle properties such as water uptake and heterogeneous chemistry.<sup>54</sup>

Phytoplankton bloom microcosms generated in the MART showed similar trends in behavior with blooms starting within 5 d, peaking within 7 to 11 d, and senescence occurring within 12 to 15 d after media addition (Figure 3). The differences in bloom peak behaviors are likely due to differences in growth rates of different phytoplankton species.<sup>57–59</sup> The range of biological conditions provides the opportunity to probe how changes in the chemical composition of seawater lead to changes in SSA composition, reactivity, and climate properties. These results will inform the assumptions required by global climate models regarding the size and single particle mixing state of nascent SSA particles.<sup>10,28</sup> In these microcosm experiments, the growth and subsequent death of the phytoplankton population resulted in changes in the concentration (Figure 4) and chemical composition (Figure 5A–C) of DOM. This change in the DOM content of seawater induced by the phytoplankton bloom created an environment that sustained the growth of marine bacteria and viruses occurring with or after the phytoplankton peak (Figures 1B and 6). Figure 1B provides an example of one microcosm experiment illustrating the dynamic nature of the three classes of marine microbes, consistent with prior marine microbiological studies.<sup>32,34,35</sup> The high concentrations of bacteria and marine viruses further alter the chemical composition of the natural organic matter through enzymatic, metabolic, and infectious processes.<sup>32,35,60–63</sup> Deviating from the conventional method of adding known compounds to synthesize a complex chemical system, the method described in this study, utilizing marine microbiology to induce realistic chemical changes in the seawater, can lead toward a better understanding of the properties and reactivity of realistic atmosphere SSA particles.

The abundances of bacteria and viruses showed distinct temporal trends in the bulk, SML, and SSA compartments (Figure 6). The abundances of bacteria ( $\sim 1 \times 10^9\ \text{L}^{-1}$ ) and viruses ( $\sim 1 \times 10^{10}\ \text{L}^{-1}$ ) were comparable to the ranges observed in the ocean before the phytoplankton bloom<sup>35</sup> as ambient seawater used to begin the microcosms, and the abundances of bacteria ( $\sim 1 \times 10^9$  to  $1 \times 10^{10}\ \text{L}^{-1}$ ) and viruses ( $\sim 1 \times 10^{10}$  to  $1 \times 10^{11}\ \text{L}^{-1}$ ) observed throughout the microcosm were also comparable to the abundances observed during oceanic bloom conditions ( $\sim 1 \times 10^{10}\ \text{L}^{-1}$  and  $\sim 1 \times 10^{11}$  to  $1 \times 10^{12}\ \text{L}^{-1}$ ).<sup>64–66</sup> Transfer of microbial species from

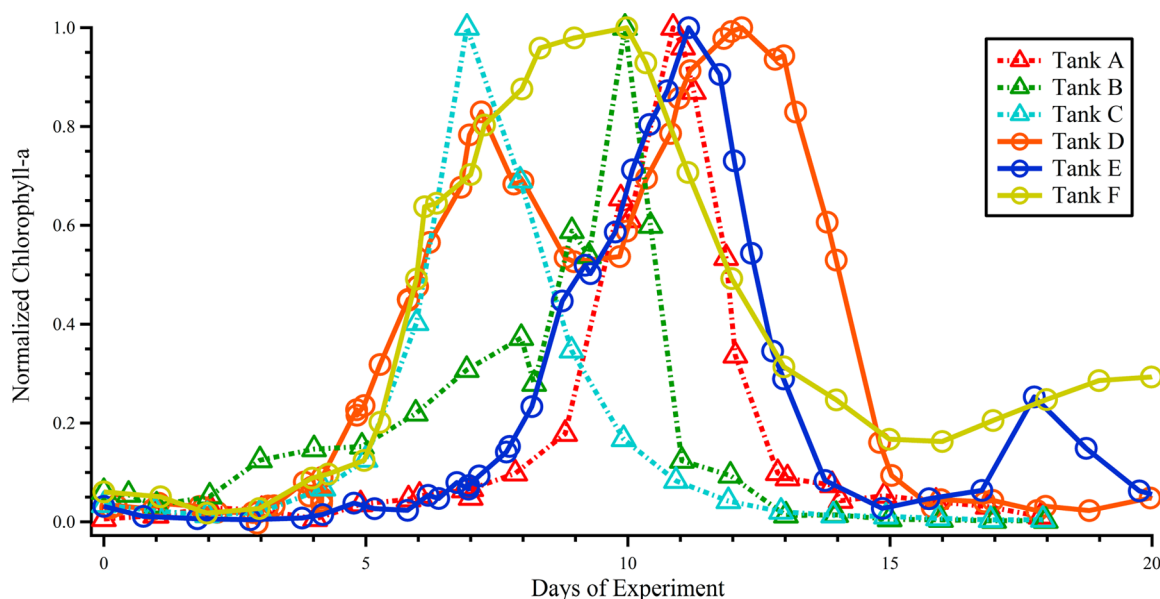


**Figure 3.** Compilation of normalized chlorophyll-*a* concentrations for the MART microcosm experiments. Despite starting with natural seawater, progression of chlorophyll-*a*, an indicator of phytoplankton biomass, behaves similarly. Dashed lines with  $\Delta$  markers and solid lines with  $\circ$  markers denote tanks with lower and higher concentration of nutrients added, respectively.

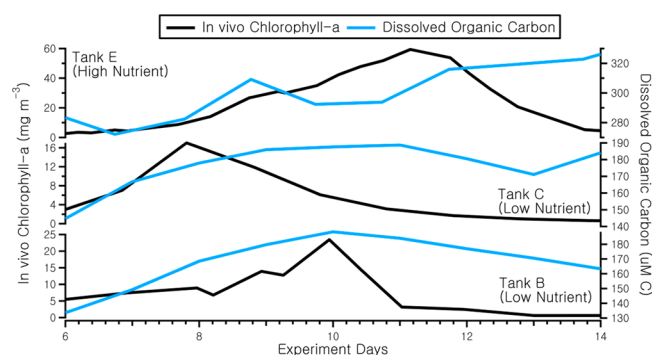


**Figure 4.** Change in concentration of DOC over the course of a microcosm experiment with a high concentration of media added (*f*/2) (Tank E, upper), and a low concentration of media added (*f*/20) (Tank C and B, center and lower, respectively).

the seawater to the aerosol phase has been previously quantified in the field<sup>67,68</sup> and is of great interest to the community as biological particles can lead to heterogeneous nucleation of ice crystals in the atmosphere<sup>67,69–73</sup> and influence cloud properties.<sup>74</sup> Detailed investigations into the source and nature of ice nucleating particles by quantifying the transfer and abundance of microorganisms in bulk seawater, SML, and SSA particles during changing seawater biological and chemical concentrations and compositions from microcosms will be presented in future publications.

**3.3. Effect in Chemical Complexity of Seawater from Phytoplankton Blooms.** Scheme 1 shows how phytoplankton, heterotrophic bacteria, and viruses contribute to and process the organics in the DOC pool of the ocean. The typical DOC concentration in the euphotic zone of the ocean is  $\sim 80 \mu\text{M C}$ <sup>75–77</sup> with some observations as high as  $250 \mu\text{M}$  in actively blooming regions.<sup>78,79</sup> The maximum DOC concentration observed in MART microcosms with *f*/20 and *f*/2 nutrient concentration were  $\sim 185 \mu\text{M C}$  and  $325 \mu\text{M C}$ , respectively (Figure 4). Note that elevated DOC concentrations immediately after nutrient addition prior to phyto-

plankton bloom in each experiment is an artifact of the addition of growth media, which contain  $\sim 12 \mu\text{M}$  of organic material ( $\text{Na}_2\text{EDTA} \cdot 2\text{H}_2\text{O}$ , vitamins  $\text{B}_1$ ,  $\text{B}_{12}$ , and H, listed in Table S2) for MART microcosms with *f*/2 concentration of media. The DOC concentrations up to  $325 \mu\text{M C}$  are above observed oceanic surface seawater conditions (typically  $80 \mu\text{M C}$ ).<sup>75–77</sup> The majority of the increase in the DOC concentration ( $175$ – $200 \mu\text{M C}$ ) is due to the media addition, where control studies of the SSA chemical composition using ATOFMS revealed small fraction ( $\sim 10\%$ ) of particles indicative of media appearing post addition and were not included in the analysis. Thus, despite the initial increase in DOC concentration that remained elevated during the microcosms with high concentration of media, the change observed in the chemistry of the SSA particles reflects the changes in the seawater from microorganisms process. Primary production of organics by photosynthetic organisms caused the concentration of DOC to increase by  $\sim 40$ – $80 \mu\text{M C}$  reaching maxima during or after the bloom of phytoplankton (Figure 4), with the eventual decrease observed in the *f*/20 microcosm experiments likely a result of heterotrophic bacterial assimilation and degradation, along with flocculation and sedimentation. Larger increases in DOC concentration were observed for the microcosms initiated with higher nutrient concentrations due to the greater abundance of the phytoplankton.

To characterize the evolution of DOM over the course of the microcosm due to the marine microbiology, fluorescence EEM measurements of the bulk seawater were performed. The fluorescent regions indicative of humic-like (excitation/emission ranges:  $360/445$ – $460 \text{ nm}$ ,  $260/425$ – $475 \text{ nm}$ , and  $320/400$ – $420 \text{ nm}$ ) and protein-like (excitation/emission ranges:  $275/300$  and  $340 \text{ nm}$ ) organic material<sup>80</sup> increased as the phytoplankton bloom progressed, divided into three time periods: before the growth of phytoplankton (prepeak), during the bloom (peak), and after phytoplankton senescence (postpeak; Figure 5A–C). Most of the sources of fluorescent dissolved organic matter (FDOM) in marine systems are assumed to be derived from biological processes<sup>81,82</sup> such as

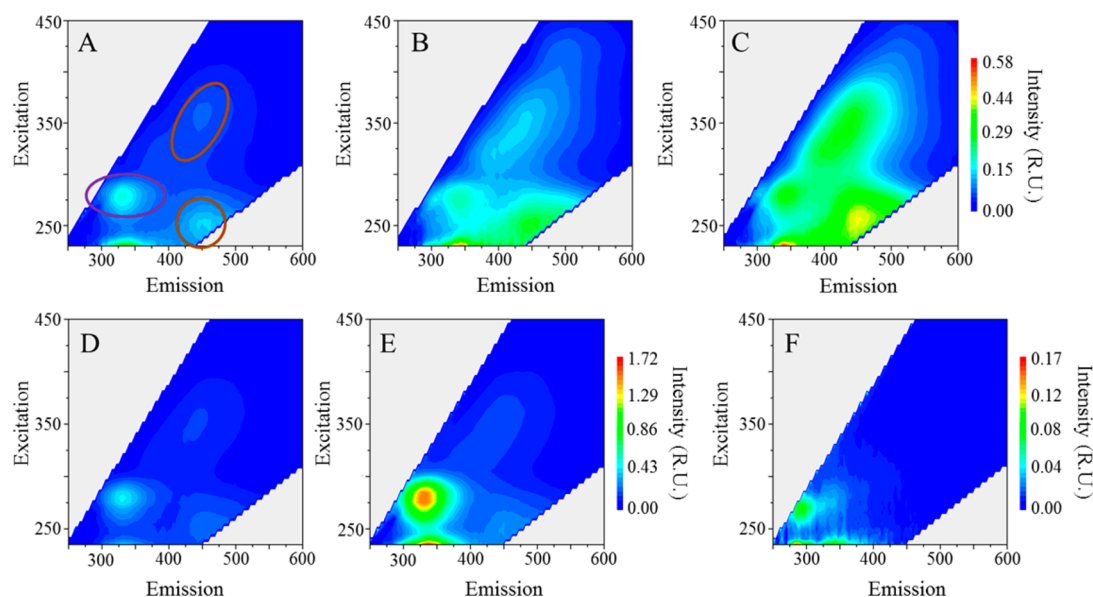


**Figure 5.** EEM spectroscopic measurement of bulk seawater at prebloom (panel A, Day 4), bloom peak (panel B, Day 11), and postpeak (panel C, Day 22) of chlorophyll-*a* for Tank E. Panels D, E, and F show the EEM measurements of bulk seawater, SML, and aerosol phase postpeak (Day 22) for Tank E. EEMs in panel C and D are of the same sample, but on different scales to highlight the enhancement in panel E from D. Humic-like substances are present at excitation/emission ranges of 360/445–460 nm, 260/425–475 nm, and 320/400–420 nm (shown in brown circles in panel A). Protein-like substances are present at 275/340 nm and 275/300 nm (region shown in purple circle in panel A).

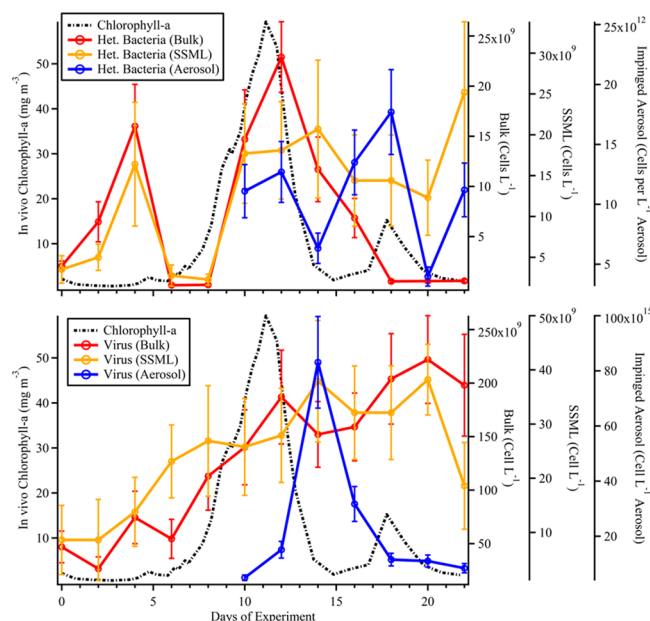
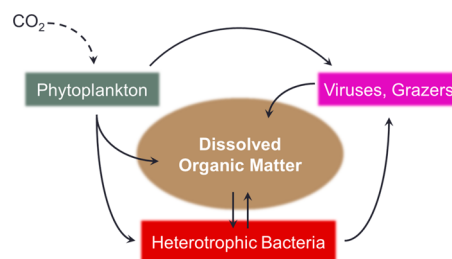


**Figure 6.** Epifluorescence microscopy counts of heterotrophic bacteria (upper) and virus (lower) in the bulk (red), SML (orange), and aerosols (blue) from an example microcosm experiment (Tank E).

byproducts of bacterial metabolism.<sup>83–85</sup> This assumption correlates well with the EEM results detailed above. The fluorescent species detected in the bulk seawater were concentrated in the SML (Figure 5D,E) likely through scavenging of surface active compounds by bubbles rising through the water column.<sup>86,87</sup> The bulk seawater has been observed in the literature to contain organic compounds such as carbohydrates, lipopolysaccharides, proteins, and lipids.<sup>36,67,88</sup> The scavenging by bubbles likely led to enrichment of these organics at the SML<sup>36,67,88,89</sup> and thus in SSA particles<sup>7,27,28</sup> in the microcosm experiments. The isolated

### Scheme 1. Simplified Schematic of the Microbial Loop Showing the Relationship between Marine Microorganisms and Dissolved Organic Matter



enclosed nature of the MART system and the plunging waterfall mechanism renews the surface between plunging waterfalls and mixes the seawater very well. However, in the enclosed area of the surface seawater in the MART, surface active compounds could build to higher concentrations than in the open ocean and thus have more pronounced changes in SSA physical and chemical composition than would occur in under similar biological conditions in the marine environment. However, while the high phytoplankton density reliably obtained in the microcosm experiments led to greater concentrations of oceanic relevant organic content than typical marine bloom conditions,<sup>72,73</sup> the microcosms provided easily measurable links between seawater biological activity and SSA composition. In future studies, microcosms with more oceanic relevant level of biological activity that mimic the ocean will be examined.

**3.4. Changes in Chemical Composition of Sea Spray Aerosol over the Microcosm.** The chemical composition of SSA particles sampled using ATOFMS were divided into three time periods discussed previously for a typical microcosm experiment (Tank E from Figure 3, for example). Period 1 corresponds to ATOFMS measurements from the prepeak (day 0) conditions. Periods 2 and 3 average ATOFMS measure-



ments corresponding to the phytoplankton bloom peak (days 9–12) and postpeak (13–22), respectively. Inorganic particles become enriched with biogenically derived organics over the course of the microcosm, which can be traced by ion markers such as  $^{26}\text{CN}^-$ ,  $^{42}\text{CNO}^-$ ,  $^{43}\text{HCNO}^+$ / $\text{C}_3\text{H}_2\text{O}^+$ , and  $^{77}\text{C}_6\text{H}_5^+$ . The top panel of Figure 7 shows relative intensities of organic

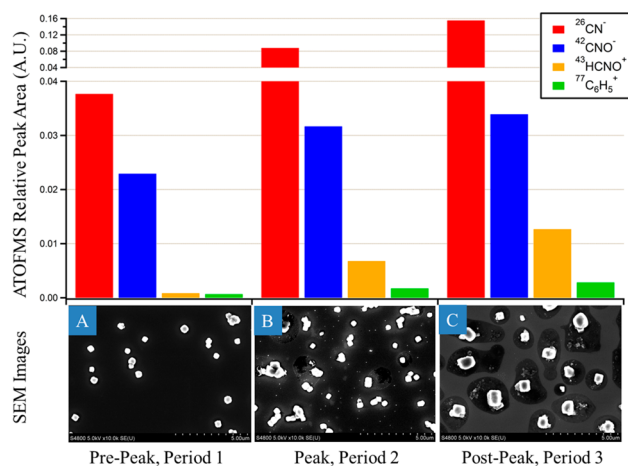


**Figure 7.** (upper) Average ATOFMS relative peak area to total area intensities of select organic ion markers in inorganic salt particles from the phytoplankton bloom during the prepeak (growth, day 0, period 1), peak (days 9–12, period 2), and postpeak (death, days 13–22, period 3) periods of the Tank E microcosm. (lower) SEM images of SSA particles (0.56 to 1.0  $\mu\text{m}$  aerodynamic diameter) observed for prepeak (day 0, panel A), peak (day 11, panel B), and postpeak (day 28, panel C) bloom periods.

ion markers to total ion intensities in the inorganic salt particles from the three designated periods, illustrating the significant organic enrichment observed after the peak of phytoplankton. Increases in the intensities of organic markers were coincident with an increase of seawater DOC concentration as the microcosm experiment progressed. While a previous study has observed a time lag between chlorophyll-*a* concentrations from satellite measurements and organic matter enrichment in ambient marine aerosol,<sup>90</sup> this study illustrates that the increases in the organic enrichment of SSA particles started to occur during the phytoplankton bloom (period 2) and become most significant after the peak in phytoplankton (period 3; Figure 7). The relationship between the dynamics of organic species in seawater and SSA mixing state will be discussed in future publications.

In addition to online measurements of SSA composition, off-line SEM measurements were performed of SSA particles with aerodynamic diameters between 0.56 and 1.0  $\mu\text{m}$  collected using a MOUDI sampler. Prior to the phytoplankton bloom (prepeak, period 1 in Figure 7), SSA particles with a strong sodium chloride signal measured by ATOFMS showed small intensities of biogenically derived organic markers. Corresponding microscopy measurements show that the morphology of the SSA particles in this size range were cubic, indicative of salt particles with low organic and water content (Figure 7A). As the bloom progressed to the peak (peak, period 2 in Figure 7), the intensities of organic markers in spectra from SSA started to increase, and a residue around the cubic salts started to appear, which has been previously observed to be organic in nature (Figure 7B and C).<sup>28,30</sup> During phytoplankton senescence (postpeak, period 3 in Figure 7), the organic residue around the

salt core became one of the dominant features in the microscopic analysis of SSA particles, corresponding to a significant increase in the intensities of the organic markers in the ATOFMS generated spectra. These results demonstrate that the approach described herein is capable of producing the chemical complexity of SSA particles whose composition varies in response to microcosm conditions. By varying microcosm conditions, it is possible to perform fundamental molecular-level studies of the heterogeneous reactivity of trace gases with aerosol particles.<sup>17,23</sup> By utilizing an aerosol flow tube reactor, the reactivity of SSA particles mixed with the complex combination of organic species produced by the microcosms will be compared to typical surfactant mimics such as sodium dodecyl sulfate<sup>24–26</sup> in future publications.

Spectroscopic measurements of organic material in the bulk, SML, and SSA particles were made to examine the selective partitioning of organic material (i.e., humic and protein-like substances) from the bulk seawater to the SML and subsequent organic enrichment in SSA particles. EEM spectroscopic measurements of the bulk seawater, SML, and the SSA particles postpeak of the phytoplankton bloom (Figure SD–F, respectively) show that the organic species synthesized in the water such as protein-like substances are enriched at the SML as well as the SSA particles. A more detailed examination of the temporal trends and the transfer of the organic species will be presented in the future.

The microcosm studies showed a clear lag between chlorophyll-*a* and organic enrichment in SSA particles, peaking after the phytoplankton (period 3). The overall trend of the organic enrichment of SSA particles occurring after the peak in phytoplankton proves that the biological processes must be considered to understand the organic enrichment in the SSA. This demonstrates the ability to recreate the complex biological conditions observed in the real world in a lab setting. The ability to replicate the chemical and biological complexity of seawater in the isolated laboratory setting will allow for more detailed physicochemical investigations of the mechanism by which organic material is enriched in SSA particles, which can further guide future marine field studies and global models.

To probe the heterogeneous reactivities of SSA particles with gas-phase pollutants such as nitric acid,<sup>91,92</sup> it is crucial to simulate the surface composition of such particles in the laboratory. The interfacial composition strongly depends on properly producing the seawater biological processes as well as physical production mechanisms as demonstrated in this study. The most critical step involves producing the proper bubble size distributions as these will selectively scavenge organic species from the water column<sup>86</sup> and ultimately break at the sea surface, producing a very specific surface composition, which will control particle reactivity.

#### 4. CONCLUSION

Here we describe a method for producing realistic SSA particles in the laboratory through the natural synthesis and subsequent chemical processing of organic compounds by marine microorganisms. This study demonstrates that the particles generated in the MART are similar to ambient particles measured during onshore flow at a coastal sampling site in the size range sampled by ATOFMS (0.3 to 3.0  $\mu\text{m}$ ).

Adapting a MART system as a photobioreactor allows one to form a vast array of organic species such as those occurring in the ocean to study the influence on SSA physicochemical properties. With unconstrained starting conditions, the



temporal behavior of the experiments showed a reasonable level of variability with blooms starting within 5 d, peaking within 7–11 d, and becoming senescent within 12–15 d of media addition. The variance in the peaks in chlorophyll-*a* concentrations that serve as a metric for phytoplankton biomass are likely due to different growth rates of phytoplankton species and nutrient concentrations. Quantitative measurements of cell counts using epifluorescence microscopy throughout the microcosm illustrate that the concentrations of heterotrophic bacteria and viruses are dynamic, increasing after the peak of phytoplankton in the bulk, SML, and aerosol phase with distinct temporal behavior in the three compartments. EEM spectroscopic measurements during the period of phytoplankton senescence in a microcosm showed that the SSA organic composition was similar to the SML, which was enriched in biological material, that is, protein-like substances, relative to the concentrations in the bulk. It is crucial to further understand the partitioning and transfer of biogenic particles and organic matter to the atmosphere as they modify physicochemical processes of SSA such as heterogeneous reactivity and affect climate-relevant processes such as ice nucleation and cloud formation.

The overall concentration and spectroscopic analysis of the DOC present in bulk seawater illustrate that the seawater became more chemically complex as the humic and protein-like species in FDOM and the DOC concentrations increased over the course of the microcosm experiments. The increase in FDOM and the overall DOC concentration in seawater are in good agreement with the assumption that the source of these organics are from biological processes. As the microcosm progressed, the SSA particles became enriched with organic species as observed from the increase in intensities of biogenically derived organic markers in ATOFMS measurements. In addition to the organic enrichment observed through mass spectrometry, the amount of residue indicative of organic material around the inorganic core of SSA particles increased as the bloom progressed. Specifically, the time lag in which the SSA particles showed a maximum in organic enrichment was observed to be between 4 and 10 d (between periods 2 and 3). The impact of this enrichment on particle properties and heterogeneous reactivity will be shown in future publications.

The approach developed in this study provides for more detailed physicochemical investigations of the mechanisms by which the chemical composition of SSA properties becomes changed above the surface of the ocean. Further, this new approach replicates the chemical complexity of SSA particles, producing a representative blend of inorganic and organic molecules in the particles that will control interfacial processes such as heterogeneous chemical reactions, water uptake, light scattering, and cloud properties of SSA.

## ■ ASSOCIATED CONTENT

### Supporting Information

The Supporting Information is available free of charge on the ACS Publications website at DOI: [10.1021/acs.jpca.5b03488](https://doi.org/10.1021/acs.jpca.5b03488).

Information on the MART photobioreactor microcosm method including oceanic conditions at the time of sampling seawater for microcosms, components of Guillard's *f* medium, as well as chlorophyll-*a* data surrounding Bodega Bay at the time of sampling, and further seawater and SSA particle measurements from the microcosm (PDF)

## ■ AUTHOR INFORMATION

### Corresponding Author

\*Phone: 858-822-5312. E-mail: [kprather@ucsd.edu](mailto:kprather@ucsd.edu).

### Present Addresses

△School of Public Health, University of Michigan.

▽National Institute Oceanography and Experimental Geophysics, Trieste, Italy.

### Author Contributions

The manuscript was written through contributions of all authors. All authors have given approval to the final version of the manuscript.

### Funding

This study was funded by the Center for Aerosol Impacts on Climate and Environment (CAICE), an NSF Center for Chemical Innovation (CHE-1305427) and through support from an endowment for the Distinguished Chair in Atmospheric Chemistry at the Univ. of California, San Diego.

### Notes

The authors declare no competing financial interest.

## ■ ACKNOWLEDGMENTS

The authors would like to thank R. Pomeroy, T. Bertram, O. Laskina, and all the collaborators involved. The authors would also like to acknowledge Bodega Marine Reserve, Univ. of California Davis, and UC Natural Reserve System.

## ■ ABBREVIATIONS

SSA, sea spray aerosols; ATOFMS, aerosol time-of-flight mass spectrometry; DOC, dissolved organic carbon; MART, marine aerosol reference tank; SLPM, standard liters per minute

## ■ REFERENCES

- (1) Molina, M. J.; Rowland, F. S. Stratospheric Sink for Chlorofluoromethanes - Chlorine Atomic-Catalysed Destruction of Ozone. *Nature* **1974**, *249*, 810–812.
- (2) Abbatt, J. P. D.; Molina, M. J. Status of Stratospheric Ozone Depletion. *Annual Review of Energy and the Environment* **1993**, *18*, 1–29.
- (3) Prenni, A. J.; Tolbert, M. A. Studies of Polar Stratospheric Cloud Formation. *Acc. Chem. Res.* **2001**, *34*, 545–553.
- (4) Tolbert, M. A.; Rossi, M. J.; Malhotra, R.; Golden, D. M. Reaction of Chlorine Nitrate with Hydrogen Chloride and Water at Antarctic Stratospheric Temperatures. *Science* **1987**, *238*, 1258–1260.
- (5) Abbatt, J. P. D.; Molina, M. J. Heterogeneous Interactions of ClONO<sub>2</sub> and HCl on Nitric-Acid Trihydrate at 202-K. *J. Phys. Chem.* **1992**, *96*, 7674–7679.
- (6) Deshler, T. A Review of Global Stratospheric Aerosol: Measurements, Importance, Life Cycle, and Local Stratospheric Aerosol. *Atmos. Res.* **2008**, *90*, 223–232.
- (7) Lewis, E. R.; Schwartz, S. E. *Sea Salt Aerosol Production: Mechanisms, Methods, Measurements and Models - a Critical Review*; Geophysical Monograph Series; American Geophysical Union: Washington, DC, 2004; Vol. 152. [10.1029/GM152](https://doi.org/10.1029/GM152).
- (8) Prather, K. A.; Hatch, C. D.; Grassian, V. H. Analysis of Atmospheric Aerosols. *Annu. Rev. Anal. Chem.* **2008**, *1*, 485–514.
- (9) Blanchard, D. C.; Woodcock, A. H. Bubble Formation and Modification in the Sea and Its Meteorological Significance. *Tellus* **1957**, *9*, 145–158.
- (10) de Leeuw, G.; Andreas, E. L.; Angelova, M. D.; Fairall, C. W.; Lewis, E. R.; O'Dowd, C.; Schulz, M.; Schwartz, S. E. Production Flux of Sea Spray Aerosol. *Rev. Geophys.* **2011**, *49*. [10.1029/2010RG000349](https://doi.org/10.1029/2010RG000349)
- (11) Tsigaridis, K.; Koch, D.; Menon, S. Uncertainties and Importance of Sea Spray Composition on Aerosol Direct and Indirect

Effects. *Journal of Geophysical Research-Atmospheres* **2013**, *118*, 220–235.

(12) O'Dowd, C. D.; Facchini, M. C.; Cavalli, F.; Ceburnis, D.; Mircea, M.; Decesari, S.; Fuzzi, S.; Yoon, Y. J.; Putaud, J. P. Biogenically Driven Organic Contribution to Marine Aerosol. *Nature* **2004**, *431*, 676–680.

(13) Saxena, P.; Hildemann, L. M.; McMurry, P. H.; Seinfeld, J. H. Organics Alter Hygroscopic Behavior of Atmospheric Particles. *J. Geophys. Res.* **1995**, *100*, 18755–18770.

(14) Cruz, C. N.; Pandis, S. N. Deliquescence and Hygroscopic Growth of Mixed Inorganic-Organic Atmospheric Aerosol. *Environ. Sci. Technol.* **2000**, *34*, 4313–4319.

(15) Moehler, O.; Benz, S.; Saathoff, H.; Schnaiter, M.; Wagner, R.; Schneider, J.; Walter, S.; Ebert, V.; Wagner, S. The Effect of Organic Coating on the Heterogeneous Ice Nucleation Efficiency of Mineral Dust Aerosols. *Environ. Res. Lett.* **2008**, *3*, 025007.

(16) Cziczo, D. J.; DeMott, P. J.; Brooks, S. D.; Prenni, A. J.; Thomson, D. S.; Baumgardner, D.; Wilson, J. C.; Kreidenweis, S. M.; Murphy, D. M. Observations of Organic Species and Atmospheric Ice Formation. *Geophys. Res. Lett.* **2004**, *31*, L12116.

(17) McNeill, V. F.; Patterson, J.; Wolfe, G. M.; Thornton, J. A. The Effect of Varying Levels of Surfactant on the Reactive Uptake of  $\text{N}_2\text{O}_5$  to Aqueous Aerosol. *Atmos. Chem. Phys.* **2006**, *6*, 1635–1644.

(18) Ryder, O. S.; Ault, A. P.; Cahill, J. F.; Guasco, T. L.; Riedel, T. P.; Cuadra-Rodriguez, L. A.; Gaston, C. J.; Fitzgerald, E.; Lee, C.; Prather, K. A.; et al. On the Role of Particle Inorganic Mixing State in the Reactive Uptake of  $\text{N}_2\text{O}_5$  to Ambient Aerosol Particles. *Environ. Sci. Technol.* **2014**, *48*, 1618–1627.

(19) Bogdan, A.; Molina, M. J. Aqueous Aerosol May Build up an Elevated Upper Tropospheric Ice Supersaturation and Form Mixed-Phase Particles after Freezing. *J. Phys. Chem. A* **2010**, *114*, 2821–2829.

(20) Salcedo, D.; Molina, L. T.; Molina, M. J. Homogeneous Freezing of Concentrated Aqueous Nitric Acid Solutions at Polar Stratospheric Temperatures†. *J. Phys. Chem. A* **2001**, *105*, 1433–1439.

(21) Salcedo, D.; Molina, L. T.; Molina, M. J. Nucleation Rates of Nitric Acid Dihydrate in 1:2  $\text{HNO}_3/\text{H}_2\text{O}$  Solutions at Stratospheric Temperatures. *Geophys. Res. Lett.* **2000**, *27*, 193–196.

(22) Molina, M. J.; Molina, L. T.; Kolb, C. E. Gas-Phase and Heterogeneous Chemical Kinetics of the Troposphere and Stratosphere. *Annu. Rev. Phys. Chem.* **1996**, *47*, 327–367.

(23) You, Y.; Smith, M. L.; Song, M.; Martin, S. T.; Bertram, A. K. Liquid-Liquid Phase Separation in Atmospherically Relevant Particles Consisting of Organic Species and Inorganic Salts. *Int. Rev. Phys. Chem.* **2014**, *33*, 43–77.

(24) Abbatt, J. P. D.; Lee, A. K. Y.; Thornton, J. A. Quantifying Trace Gas Uptake to Tropospheric Aerosol: Recent Advances and Remaining Challenges. *Chem. Soc. Rev.* **2012**, *41*, 6555–6581.

(25) Finlayson-Pitts, B. J. Reactions at Surfaces in the Atmosphere: Integration of Experiments and Theory as Necessary (but Not Necessarily Sufficient) for Predicting the Physical Chemistry of Aerosols. *Phys. Chem. Chem. Phys.* **2009**, *11*, 7760–7779.

(26) Krueger, B. J.; Grassian, V. H.; Iedema, M. J.; Cowin, J. P.; Laskin, A. Probing Heterogeneous Chemistry of Individual Atmospheric Particles Using Scanning Electron Microscopy and Energy-Dispersive X-Ray Analysis. *Anal. Chem.* **2003**, *75*, 5170–5179.

(27) Collins, D. B.; Zhao, D. F.; Ruppel, M. J.; Laskina, O.; Grandquist, J. R.; Modini, R. L.; Stokes, M. D.; Russell, L. M.; Bertram, T. H.; Grassian, V. H.; et al. Direct Aerosol Chemical Composition Measurements to Evaluate the Physicochemical Differences between Controlled Sea Spray Aerosol Generation Schemes. *Atmos. Meas. Tech.* **2014**, *7*, 3667–3683.

(28) Prather, K. A.; Bertram, T. H.; Grassian, V. H.; Deane, G. B.; Stokes, M. D.; DeMott, P. J.; Aluwihare, L. I.; Palenik, B. P.; Azam, F.; Seinfeld, J. H.; et al. Bringing the Ocean into the Laboratory to Probe the Chemical Complexity of Sea Spray Aerosol. *Proc. Natl. Acad. Sci. U. S. A.* **2013**, *110*, 7550–7555.

(29) Stokes, M. D.; Deane, G. B.; Prather, K.; Bertram, T. H.; Ruppel, M. J.; Ryder, O. S.; Brady, J. M.; Zhao, D. A Marine Aerosol Reference Tank System as a Breaking Wave Analogue for the

Production of Foam and Sea-Spray Aerosols. *Atmos. Meas. Tech.* **2013**, *6*, 1085–1094.

(30) Ault, A. P.; Moffet, R. C.; Baltrusaitis, J.; Collins, D. B.; Ruppel, M. J.; Cuadra-Rodriguez, L. A.; Zhao, D.; Guasco, T. L.; Ebben, C. J.; Geiger, F. M.; et al. Size-Dependent Changes in Sea Spray Aerosol Composition and Properties with Different Seawater Conditions. *Environ. Sci. Technol.* **2013**, *47*, S603–S612.

(31) Teeling, H.; Fuchs, B. M.; Becher, D.; Klockow, C.; Gardebrecht, A.; Bennke, C. M.; Kassabgy, M.; Huang, S.; Mann, A. J.; Waldmann, J.; et al. Substrate-Controlled Succession of Marine Bacterioplankton Populations Induced by a Phytoplankton Bloom. *Science* **2012**, *336*, 608–611.

(32) Pomeroy, L. R.; Williams, P. J. I.; Azam, F.; Hobbie, J. E. The Microbial Loop. *Oceanography* **2007**, *20*, 28–33.

(33) Azam, F.; Fenchel, T.; Field, J. G.; Gray, J. S.; Meyerreil, L. A.; Thingstad, F. The Ecological Role of Water-Column Microbes in the Sea. *Mar. Ecol.: Prog. Ser.* **1983**, *10*, 257–263.

(34) Azam, F.; Smith, D. C.; Steward, G. F.; Hagstrom, A. Bacteria - Organic-Matter Coupling and Its Significance for Oceanic Carbon Cycling. *Microb. Ecol.* **1994**, *28*, 167–179.

(35) Azam, F.; Malfatti, F. Microbial Structuring of Marine Ecosystems. *Nat. Rev. Microbiol.* **2007**, *5*, 782–791.

(36) Hessen, D. O.; Tranvik, L. J. *Aquatic Humic Substances: Ecology and Biogeochemistry*; Springer-Verlag: Berlin, Germany, 1998.

(37) Bouvet, M.; Hoepffner, N.; Dowell, M. D. Parameterization of a Spectral Solar Irradiance Model for the Global Ocean Using Multiple Satellite Sensors. *J. Geophys. Res.* **2002**, *107*, 10.1029/2001JC001126.

(38) Brown, T. E.; Richardson, F. L. The Effect of Growth Environment on the Physiology of Algae: Light Intensity<sup>12</sup>. *J. Phycol.* **1968**, *4*, 38–54.

(39) Sorokin, C.; Krauss, R. W. The Effects of Light Intensity on the Growth Rates of Green Algae. *Plant Physiol.* **1958**, *33*, 109–113.

(40) Guillard, R. R.; Ryther, J. H. Studies of Marine Planktonic Diatoms. I. *Cyclotella* Nana Hustedt, and *Detonula* Confervacea (Cleve) Gran. *Can. J. Microbiol.* **1962**, *8*, 229.

(41) Guillard, R. R. L. *Culture of Phytoplankton for Feeding Marine Invertebrates* **1975**, *1*, 29–60.

(42) Cunliffe, M.; Engel, A.; Frka, S.; Gašparović, B.; Guitart, C.; Murrell, J. C.; Salter, M.; Stolle, C.; Upstill-Goddard, R.; Wurl, O. Sea Surface Microlayers: A Unified Physicochemical and Biological Perspective of the Air–Ocean Interface. *Prog. Oceanogr.* **2013**, *109*, 104–116.

(43) Alvarez-Salgado, X. A.; Miller, A. E. J. Simultaneous Determination of Dissolved Organic Carbon and Total Dissolved Nitrogen in Seawater by High Temperature Catalytic Oxidation: Conditions for Precise Shipboard Measurements. *Mar. Chem.* **1998**, *62*, 325–333.

(44) Noble, R. T.; Fuhrman, J. A. Use of Sybr Green I for Rapid Epifluorescence Counts of Marine Viruses and Bacteria. *Aquat. Microb. Ecol.* **1998**, *14*, 113–118.

(45) Dall'Osto, M.; Harrison, R. M.; Coe, H.; Williams, P. Real-Time Secondary Aerosol Formation During a Fog Event in London. *Atmos. Chem. Phys.* **2009**, *9*, 2459–2469.

(46) Fry, J. L.; Draper, D. C.; Barsanti, K. C.; Smith, J. N.; Ortega, J.; Winkler, P. M.; Lawler, M. J.; Brown, S. S.; Edwards, P. M.; Cohen, R. C.; et al. Secondary Organic Aerosol Formation and Organic Nitrate Yield from  $\text{NO}_3$  Oxidation of Biogenic Hydrocarbons. *Environ. Sci. Technol.* **2014**, *48*, 11944–11953.

(47) Gard, E.; Mayer, J. E.; Morrical, B. D.; Dienes, T.; Fergenson, D. P.; Prather, K. A. Real-Time Analysis of Individual Atmospheric Aerosol Particles: Design and Performance of a Portable Atoms. *Anal. Chem.* **1997**, *69*, 4083–4091.

(48) Gaston, C. J.; Furutani, H.; Guazzotti, S. A.; Coffee, K. R.; Bates, T. S.; Quinn, P. K.; Aluwihare, L. I.; Mitchell, B. G.; Prather, K. A. Unique Ocean-Derived Particles Serve as a Proxy for Changes in Ocean Chemistry. *J. Geophys. Res.* **2011**, *116*, D18310.

(49) Guasco, T. L.; Cuadra-Rodriguez, L. A.; Pedler, B. E.; Ault, A. P.; Collins, D. B.; Zhao, D.; Kim, M. J.; Ruppel, M. J.; Wilson, S. C.; Pomeroy, R. S.; et al. Transition Metal Associations with Primary

Biological Particles in Sea Spray Aerosol Generated in a Wave Channel. *Environ. Sci. Technol.* **2014**, *48*, 1324–1333.

(50) Gard, E. E.; Kleeman, M. J.; Gross, D. S.; Hughes, L. S.; Allen, J. O.; Morrical, B. D.; Fergenson, D. P.; Dienes, T.; Gälli, M. E.; Johnson, R. J.; Cass, G. R.; Prather, K. A.; et al. Direct Observation of Heterogeneous Chemistry in the Atmosphere. *Science* **1998**, *279*, 1184–1187.

(51) Kolb, C. E.; Cox, R. A.; Abbatt, J. P. D.; Ammann, M.; Davis, E. J.; Donaldson, D. J.; Garrett, B. C.; George, C.; Griffiths, P. T.; Hanson, D. R.; et al. An Overview of Current Issues in the Uptake of Atmospheric Trace Gases by Aerosols and Clouds. *Atmos. Chem. Phys.* **2010**, *10*, 10561–10605.

(52) Cloern, J. E. Phytoplankton Bloom Dynamics in Coastal Ecosystems: A Review with Some General Lessons from Sustained Investigation of San Francisco Bay, California. *Rev. Geophys.* **1996**, *34*, 127–168.

(53) Sullivan, C. W.; Arrigo, K. R.; McClain, C. R.; Comiso, J. C.; Firestone, J. Distributions of Phytoplankton Blooms in the Southern Ocean. *Science* **1993**, *262*, 1832–1837.

(54) NASA Earth Observations Chlorophyll Concentration (Aqua/Modis). [http://neo.sci.gsfc.nasa.gov/view.php?datasetId=MY1DMM\\_CHLORA](http://neo.sci.gsfc.nasa.gov/view.php?datasetId=MY1DMM_CHLORA) (accessed 16 Sept 2014).

(55) National Oceanic and Atmospheric Administration, U.S.D.o.C. Ocean. <http://www.noaa.gov/ocean.html> (accessed 29 May 2015).

(56) Yoder, J. A.; McClain, C. R.; Feldman, G. C.; Esaias, W. E. Annual Cycles of Phytoplankton Chlorophyll Concentrations in the Global Ocean: A Satellite View. *Global Biogeochemical Cycles* **1993**, *7*, 181–193.

(57) Mura, M. P.; Agusti, S. Growth Rates of Diatoms from Coastal Antarctic Waters Estimated by in Situ Dialysis Incubation. *Mar. Ecol. Prog. Ser.* **1996**, *144*, 237–245.

(58) Gilstad, M.; Sakshaug, E. Growth-Rates of 10 Diatom Species from the Barents Sea at Different Irradiances and Day Lengths. *Mar. Ecol. Prog. Ser.* **1990**, *64*, 169–173.

(59) Tang, E. P. Y. The Allometry of Algal Growth Rates. *J. Plankton Res.* **1995**, *17*, 1325–1335.

(60) Grossart, H. P.; Czub, G.; Simon, M. Algae-Bacteria Interactions and Their Effects on Aggregation and Organic Matter Flux in the Sea. *Environ. Microbiol.* **2006**, *8*, 1074–1084.

(61) Smith, D. C.; Steward, G. F.; Long, R. A.; Azam, F. Bacterial Mediation of Carbon Fluxes During a Diatom Bloom in a Mesocosm. *Deep Sea Res., Part II* **1995**, *42*, 75–97.

(62) Smith, D. C.; Simon, M.; Alldredge, A. L.; Azam, F. Intense Hydrolytic Enzyme-Activity on Marine Aggregates and Implications for Rapid Particle Dissolution. *Nature* **1992**, *359*, 139–142.

(63) Grossart, H. P.; Ploug, H. Microbial Degradation of Organic Carbon and Nitrogen on Diatom Aggregates. *Limnol. Oceanogr.* **2001**, *46*, 267–277.

(64) Bird, D. F.; Kalf, J. Empirical Relationships between Bacterial Abundance and Chlorophyll Concentration in Fresh and Marine Waters. *Can. J. Fish. Aquat. Sci.* **1984**, *41*, 1015–1023.

(65) Riemann, L.; Steward, G. F.; Azam, F. Dynamics of Bacterial Community Composition and Activity During a Mesocosm Diatom Bloom. *Appl. Environ. Microbiol.* **2000**, *66*, 578–587.

(66) Suttle, C. A. Viruses in the Sea. *Nature* **2005**, *437*, 356–361.

(67) Aller, J. Y.; Kuznetsova, M. R.; Jahns, C. J.; Kemp, P. F. The Sea Surface Microlayer as a Source of Viral and Bacterial Enrichment in Marine Aerosols. *J. Aerosol Sci.* **2005**, *36*, 801–812.

(68) Dueker, M. E.; O'Mullan, G. D. Aeration Remediation of a Polluted Waterway Increases near-Surface Coarse and Culturable Microbial Aerosols. *Sci. Total Environ.* **2014**, *478*, 184–189.

(69) Burrows, S. M.; Hoose, C.; Poeschl, U.; Lawrence, M. G. Ice Nuclei in Marine Air: Biogenic Particles or Dust? *Atmos. Chem. Phys.* **2013**, *13*, 245–267.

(70) Despres, V. R.; Huffman, J. A.; Burrows, S. M.; Hoose, C.; Safatov, A. S.; Buryak, G.; Frohlich-Nowoisky, J.; Elbert, W.; Andreae, M. O.; Pöschl, U.; Jaenicke, R.; et al. Primary Biological Aerosol Particles in the Atmosphere: A Review. *Tellus, Ser. B* **2012**, *64*, 10.3402/tellusb.v64i0.15598.

(71) Schnell, R. C.; Vali, G. Biogenic Ice Nuclei 0.1. Terrestrial and Marine Sources. *J. Atmos. Sci.* **1976**, *33*, 1554–1564.

(72) Vali, G.; Christensen, M.; Fresh, R. W.; Galyan, E. L.; Maki, L. R.; Schnell, R. C. Biogenic Ice Nuclei 0.2. Bacterial Sources. *J. Atmos. Sci.* **1976**, *33*, 1565–1570.

(73) Wolber, P. K. Bacterial Ice Nucleation. *Advances in Microbial Physiology, Vol 34* **1993**, *34*, 203–237.

(74) Sun, J.; Ariya, P. A. Atmospheric Organic and Bio-Aerosols as Cloud Condensation Nuclei (CCN): A Review. *Atmos. Environ.* **2006**, *40*, 795–820.

(75) McCarthy, M. D.; Hedges, J. I.; Benner, R. Major Bacterial Contribution to Marine Dissolved Organic Nitrogen. *Science* **1998**, *281*, 231–234.

(76) Aristegui, J.; Duarte, C. M.; Agusti, S.; Doval, M.; Alvarez-Salgado, X. A.; Hansell, D. A. Dissolved Organic Carbon Support of Respiration in the Dark Ocean. *Science* **2002**, *298*, 1967–1967.

(77) DeLong, E. F.; Preston, C. M.; Mincer, T.; Rich, V.; Hallam, S. J.; Frigaard, N. U.; Martinez, A.; Sullivan, M. B.; Edwards, R.; Brito, B. R.; Chisholm, S. W.; Karl, D. M.; et al. Community Genomics among Stratified Microbial Assemblages in the Ocean's Interior. *Science* **2006**, *311*, 496–503.

(78) Kirchman, D. L.; Suzuki, Y.; Garside, C.; Ducklow, H. W. High Turnover Rates of Dissolved Organic-Carbon During a Spring Phytoplankton Bloom. *Nature* **1991**, *352*, 612–614.

(79) Norrman, B.; Zweifel, U. L.; Hopkinson, C. S.; Fry, B. Production and Utilization of Dissolved Organic-Carbon During an Experimental Diatom Bloom. *Limnol. Oceanogr.* **1995**, *40*, 898–907.

(80) Coble, P. G. Characterization of Marine and Terrestrial Dom in Seawater Using Excitation Emission Matrix Spectroscopy. *Mar. Chem.* **1996**, *51*, 325–346.

(81) Jaffe, R.; McKnight, D.; Maie, N.; Cory, R.; McDowell, W. H.; Campbell, J. L. Spatial and Temporal Variations in DOM Composition in Ecosystems: The Importance of Long-Term Monitoring of Optical Properties. *J. Geophys. Res.* **2008**, *113*, G04032.

(82) Maie, N.; Boyer, J. N.; Yang, C.; Jaffe, R. Spatial, Geomorphological, and Seasonal Variability of C<sub>dm</sub> in Estuaries of the Florida Coastal Everglades. *Hydrobiologia* **2006**, *569*, 135–150.

(83) Nieto-Cid, M.; Alvarez-Salgado, X. A.; Perez, F. F. Microbial and Photochemical Reactivity of Fluorescent Dissolved Organic Matter in a Coastal Upwelling System. *Limnol. Oceanogr.* **2006**, *51*, 1391–1400.

(84) Shimotori, K.; Omori, Y.; Hama, T. Bacterial Production of Marine Humic-Like Fluorescent Dissolved Organic Matter and Its Biogeochemical Importance. *Aquat. Microb. Ecol.* **2009**, *58*, 55–66.

(85) Yamashita, Y.; Tanoue, E. Production of Bio-Refractory Fluorescent Dissolved Organic Matter in the Ocean Interior. *Nat. Geosci.* **2008**, *1*, 579–582.

(86) Blanchard, D. C. Bubble Scavenging and Water-to-Air Transfer of Organic Material in Sea. *Advances in Chemistry Series* **1975**, *145*, 360–387.

(87) Keene, W. C.; Maring, H.; Maben, J. R.; Kieber, D. J.; Pszenny, A. A. P.; Dahl, E. E.; Izaguirre, M. A.; Davis, A. J.; Long, M. S.; Zhou, X.; Smoydzin, L.; Sander, R.; et al. Chemical and Physical Characteristics of Nascent Aerosols Produced by Bursting Bubbles at a Model Air-Sea Interface. *J. Geophys. Res.* **2007**, *112*, D2120.

(88) Carlson, D. J. Dissolved Organic Materials in Surface Microlayers - Temporal and Spatial Variability and Relation to Sea State. *Limnol. Oceanogr.* **1983**, *28*, 415–431.

(89) Cunliffe, M.; Upstill-Goddard, R. C.; Murrell, J. C. Microbiology of Aquatic Surface Microlayers. *Fems Microbiology Reviews* **2011**, *35*, 233–246.

(90) Rinaldi, M.; Fuzzi, S.; Decesari, S.; Marullo, S.; Santolieri, R.; Provenza, A.; von Hardenberg, J.; Ceburnis, D.; Vaishya, A.; O'Dowd, C. D.; Facchini, M. C.; et al. Is Chlorophyll-a the Best Surrogate for Organic Matter Enrichment in Submicron Primary Marine Aerosol? *Journal of Geophysical Research-Atmospheres* **2013**, *118*, 4964–4973.

(91) Ault, A. P.; Guasco, T. L.; Baltrusaitis, J.; Ryder, O. S.; Trueblood, J. V.; Collins, D. B.; Ruppel, M. J.; Cuadra-Rodriguez, L. A.; Prather, K. A.; Grassian, V. H. Heterogeneous Reactivity of Nitric



Acid with Nascent Sea Spray Aerosol: Large Differences Observed between and within Individual Particles. *J. Phys. Chem. Lett.* **2014**, *5*, 2493–2500.

(92) Ault, A. P.; Guasco, T. L.; Ryder, O. S.; Baltrusaitis, J.; Cuadra-Rodriguez, L. A.; Collins, D. B.; Ruppel, M. J.; Bertram, T. H.; Prather, K. A.; Grassian, V. H. Inside Versus Outside: Ion Redistribution in Nitric Acid Reacted Sea Spray Aerosol Particles as Determined by Single Particle Analysis. *J. Am. Chem. Soc.* **2013**, *135*, 14528–14531.